www.czasopisma.pan.pl PAN POLSKA AKADEMIA NAUK www.journals.pan.pl

jet INTL JOURNAL OF ELECTRONICS AND TELECOMMUNICATIONS, 2023, VOL. 69, NO. 3, PP. 455-460
Manuscript received June 3, 2023; revised July, 2023. DOI: 10.24425/ijet.2023.144383

# A Tiny 2.4 GHz Monopole Water Antenna

Koyu Chinen, and Ichiko Kinjo

***Abstract*—We designed, fabricated, and evaluated a monopole water antenna (WA) filled with pure water. A 2.4 GHz patch antenna (PA) was used for measurement comparison, and the current density distribution and 3D field strength radiation distribution and reflection coefficient of the PA had a fundamental mode and a higher-order mode at 3.5 GHz, whose polarization was 90 degrees different. The 2.4 GHz monopole WA could receive only the fundamental mode of the PA. The 3.5 GHz WA could receive the higher-order mode of the PA by rotating the WA by 90 degrees. The transmission coefficient of the 2.4 GHz WA decreased with the square of the spacing, similar to the spatial propagation characteristics of electromagnetic waves. Almost the same results could be expected if planar or three-dimensional antennas were used instead of monopole electrodes.**

***Keywords*—water antenna; polar molecule; S-parameter; monopole antenna; underwater wireless communication**

## I. Introduction

WATER antennas are characterized by their small size and flexible shape, which are achieved by taking advantage of the high permittivity of water. Therefore, water antennas have been widely studied for wireless communications in seawater and freshwater because of their excellent affinity with liquids. Many reports have been on monopole-type water antennas because of their simple structure [1-27] and evaluated the reflection coefficient $S_{11}$ by changing the electrode structure and liquid structures (aqueous solution material and shape) [5, 11, 23]. Most of the proposed water antenna structures are open-end, which makes their size rather large [3, 9, 14, 17, 21, 26]. There are many reports on using frequencies below 1 GHz and a few hundred MHz in the case of seawater due to high attenuation rates [3, 8, 9, 11, 13, 15, 16, 23]. Many research reports have investigated the changes in frequency and reflectivity of dielectric resonance caused by immersing a planar antenna, such as a patch antenna, in a liquid [2, 4, 6, 10, 14, 18, 24]. There are few detailed reports on the evaluation of transmission characteristics in the GHz band using water antennas as transmitting and receiving antennas.

In this study, we designed and fabricated a small and portable water antenna that can be used to transmit and receive high-frequency signals in the 2.4 GHz band used in wireless LANs and investigated its transmission characteristics.

## II. 2.4 GHz Band Monopole Water Antenna and Transmission Measurement System

We evaluated the 2.4 GHz monopole water antenna's characteristics and signal transmission and reception by S-parameter measurements. The configuration of the S-parameter measurement system is shown in Figure 1.

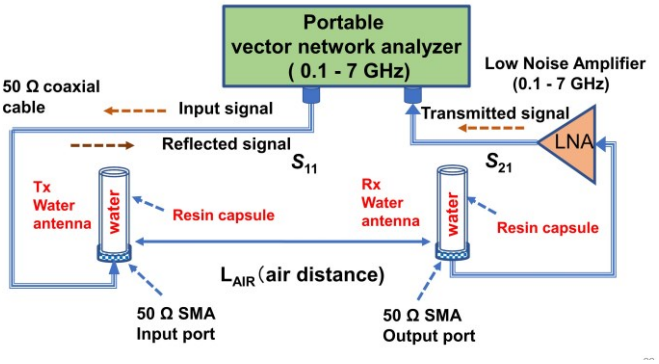


Fig. 1. Measurement system for transmission characteristics of water antennas

The reflection coefficient $S_{11}$ and transmission coefficient $S_{21}$ were calculated by measuring the reflection and transmission signals of RF signals in the 0.1 to 6 GHz band using a portable vector network analyzer (VNA) [27]. The high-frequency signal was fed from the output port of the VNA to a monopole water antenna (Tx-WA) for transmission using a 50 Ω coaxial cable. The output signal from the receiving monopole water antenna (Rx-WA) was connected to a low-noise amplifier with a bandwidth of 0.1 to 7 GHz and a gain of 20 dB, which was designed and fabricated using a coplanar line and a single-stage SiGe bipolar transistor. The output of the LNA was connected to the input port of the vector network analyzer. The measurement system was calibrated using SOLT (short, open, load, and through) terminals between the output connector of a 50 Ω coaxial cable connected to the output port of the VNA and the input port of the VNA. The measured S-parameters are expressed in complex or polar coordinates, but in this paper, they are evaluated in terms of their magnitude. cylindrical acrylonitrile butadiene styrene (ABS) resin capsule

Koyu Chinen is with GLEX, Yokohama, Japan (email: kouy.chinen@nifty.com).

Ichiko Kinjo is with Information and Communication System Engineering Dept., National Institute of Technology, Okinawa College, Nago, Japan (email: ichi@ Okinawa-ct.ac.jp).

The 2.4 GHz band monopole water antenna consists of a with an inner diameter of 8 mm and an outer diameter of 10 mm, and a 50 Ω SMA (Sub Miniature Type A) electrode. The central signal pin of the SMA electrode was placed inside the capsule, and the capsule was filled with pure water purified by ion exchange resin and reverse osmosis membrane. The capsule length $L_{WA}$ is 25 mm or 50 mm. A photograph of the external appearance is shown in Figure 2. The impedance matching between pure water and SMA electrodes in the 2-4 GHz frequency range was investigated by varying the length of the center signal pin of the SMA electrode and measuring the frequency of the minimum value of the reflection coefficient $S_{11}$. The measured and simulated electromagnetic field values are shown in Figure 3. The signal pin length of the impedance-matched SMA electrode at 2.4 GHz was 8 mm. The minimum value of $S_{11}$ is relatively large, about -5 dB. When the size and shape of the ground were changed to enclose the lower part of the signal pin of the SMA electrode [20], $S_{11}$ was reduced to less than -10 dB, but the transfer coefficient $S_{21}$ also decreased. One possible cause of this is the effect of changes in the current density distribution of the signal pins. A flat SMA connector flange was therefore used for the ground.

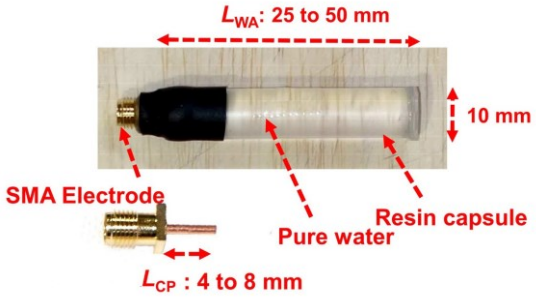


Fig. 2. Appearance of 2.4 GHz band monopole water antenna

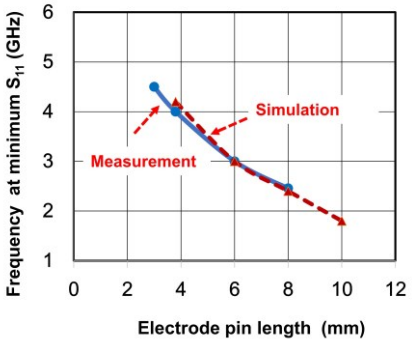


Fig. 3. Relationship between the electrode pin length of the monopole water antenna and the frequency at which the minimum value of $S_{11}$ of the monopole water antenna is reached

## III. Design, Fabrication, and Characterization of 2.4 GHz Band Patch Antennas

To evaluate the transmission and reception characteristics of the 2.4 GHz band monopole water antenna, we designed and fabricated a 2.4 GHz band patch antenna as a reference antenna for comparison. Patch antennas are suitable as reference antennas for evaluating the antenna characteristics of designed and fabricated monopole water antennas because they are directional, have a narrow bandwidth frequency response, and have stable characteristics. The 2.4 GHz band patch antenna was fabricated using a 36 μm double-sided copper-clad FR-4 (Flame Retardant Type 4) substrate with a thickness of 1.6 mm. We used an electromagnetic simulator AXIEM [28] to determine the antenna length $L_{PAL}$ and width $L_{PAW}$, for which the reflection coefficient $S_{11}$ at 2.4 GHz is a minimum. The feeder line was designed as a 50 Ω MSL (Micro Strip Line), and 50 Ω SMA was used for the connectors.

The current density distribution and electric field intensity radiation pattern ($E_\theta$ and $E\varphi$) of the 2.4 GHz band patch antenna obtained by electromagnetic field simulation are shown in Figure 4. The current flows in the direction along $L_{PAL}$ (X-axis direction), and the vertical ($E_\theta$) and horizontal ($E\varphi$) polarization components of the radiated electric field intensity of the electromagnetic wave generated by this current are shown. The results of the measured and simulated values of the reflection coefficient $S_{11}$ obtained from the electromagnetic field simulation are shown in Figure 5. In the 0.1 to 6 GHz frequency range, in addition to the fundamental frequency of 2.4 GHz, higher-order mode frequencies appear at 3.5 GHz and 4.5 GHz.

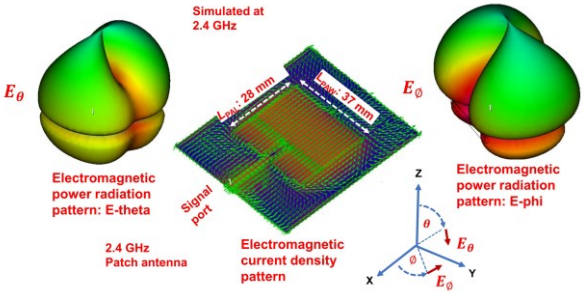


Fig. 4. Current density distribution and electric field intensity radiation pattern of 2.4 GHz patch antenna

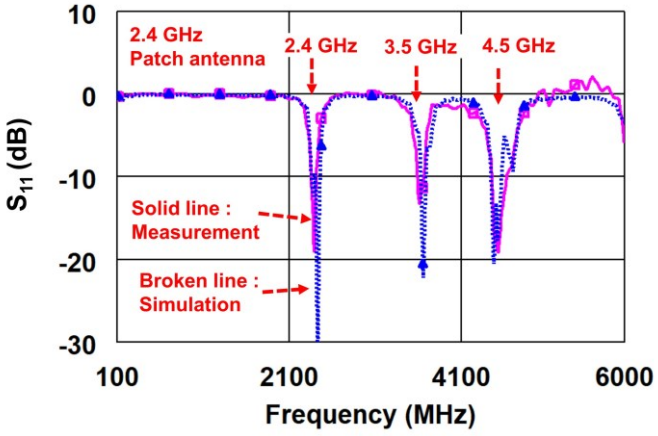


Fig. 5. Measured and simulated $S_{11}$ values for the 2.4 GHz patch antenna

The current density distribution and electric field intensity radiation pattern at 3.5 GHz for the higher-order modes are shown in Figure 6. The current density distribution is bisected at the antenna width $L_{PAW}$, indicating resonance of the second higher-order mode ($TE_{02}$). The current shows a direction rotated by 90 degrees relative to the 2.4 GHz fundamental resonance mode $TE_{10}$, and the field strength radiation pattern ($E_\theta$) generated by the current also shows a direction rotated by 90 degrees. The electric field strength radiation pattern ($E\varphi$) divided into two parts by the resonance mode divided into two parts in the Y direction is shown.

The higher-order mode at 4.5 GHz represents a resonant frequency close to $TE_{12}$. Because the $TE_{10}$ mode was added to $TE_{02}$ mode, the electric field intensity radiation pattern showed the same direction as the fundamental resonance mode with $E_\theta$ rotated another 90 degrees, and the $E\varphi$ mode showed the same pattern as $TE_{02}$ mode. In this paper, the 3.5 GHz frequency is treated as a representative example of higher-order mode transmission and reception. Therefore, higher-order mode transmission and reception at 4.5 GHz will not be discussed.

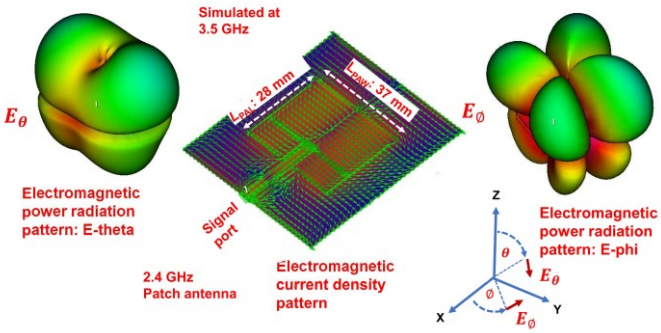


Fig. 6. Current density distribution and electric field intensity radiation pattern of the 2.4 GHz patch antenna at 3.5 GHz

## IV. Transmission and Reception Characteristics of 2.4 GHz Band Monopole Water Antennas

We measured the S-parameter reflection coefficient $S_{11}$ and transmission coefficient $S_{21}$ by placing the 2.4 GHz patch antennas at the transmitting and receiving antenna positions of the transmission measurement system (Figure 1). The measurement result is shown in Figure 7. The transmitting coefficients $S_{21}$ corresponding to the resonance frequencies of 2.4 GHz, 3.5 GHz, and 4.5 GHz, as shown in the measured value of the reflection coefficient $S_{11}$, were measured. Hence both fundamental mode and higher-order mode signals were transmitted and received. This result indicates that electromagnetic waves with different frequencies and electric field intensity patterns are transmitted and received when the transmitting and receiving antennas have the same structure and characteristics.

The reflection coefficient $S_{11}$ and transmission coefficient $S_{21}$ were measured using a 2.4 GHz patch antenna as the transmitting antenna and a 2.4 GHz monopole water antenna as the receiving antenna, as shown in Figure 8. The 2.4 GHz fundamental mode signal was received normally, but the higher-order mode signal could not be received. This is because the receiving monopole water antenna has an 8 mm electrode pin length, which optimizes the impedance to 2.4 GHz and eliminates higher-order modes. When the lengths of the resin capsule $L_{WA}$ were 25 mm and 50 mm, the transmitted signal $S_{21}$ at 2.4 GHz was slightly larger but not significantly different when a monopole water antenna with an $L_{WA}$ length of 50 mm was used as the receiving antenna.

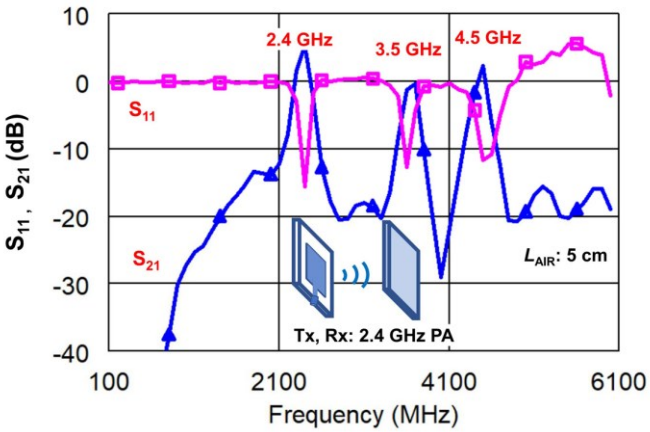


Fig. 7. Reflection coefficient $S_{11}$ and transmission coefficient $S_{21}$ measured with 2.4 GHz patch antennas

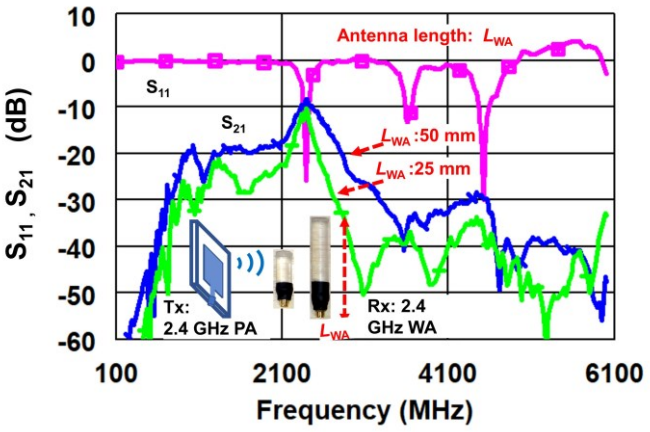


Fig. 8. Reflection coefficient $S_{11}$ (PA) and transmission coefficient $S_{21}$ measurement with 2.4 GHz band patch antenna (transmitter) and 2.4 GHz band monopole water antenna (receiver)

## V. Transmission and Reception Characteristics of 2.4 GHz Band Monopole Water Antennas

The current density distribution and electric field intensity radiation pattern ($E_\theta$ and $E\varphi$) of the 2.4 GHz band monopole water antenna in pure water obtained by electromagnetic field simulation are shown in Figure 9. The current density increases from the top (tip) of the signal pin toward the bottom, indicating the current density distribution of a typical monopole antenna. The electric field intensity radiation patterns ($E_\theta$ and $E\varphi$) along this current direction (X-axis direction) are shown and have the same direction as the electric field intensity radiation pattern of the 2.4 GHz band patch antenna shown in Figure 4.

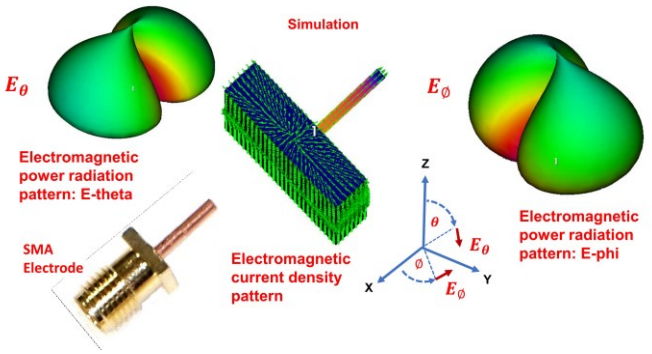


Fig. 9. Current density distribution and electric field intensity pattern of the 2.4 GHz band monopole water antenna

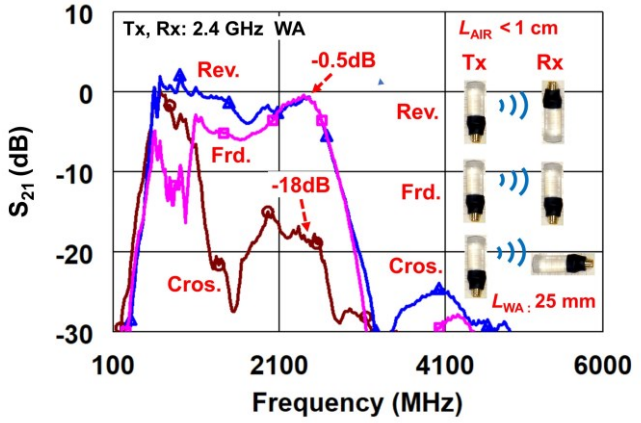


Fig. 10. Transmission coefficient $S_{21}$ measurement for the 2.4 GHz band monopole water antennas with different antenna angles during the measurements

Figure 10 shows the results of the $S_{21}$ transmission coefficient measurement using a 2.4 GHz monopole water antenna as the transmitting and receiving antennas. The direction of the receiving antenna was changed to forward (Forward), reverse (Reverse), and right-angle crossing (Cross) as the direction of the transmitting antenna. The measurement result of the $S_{21}$ transmission coefficient at 2.4 GHz showed no significant difference between the forward and reverse counterparts but a decrease of about 17 dB for the right-angle crossing counterparts. This is because, as shown in Figure 9, the electric field intensity radiation pattern ($E_\theta$ and $E\varphi$) of the monopole water antenna is determined by the current in the x-axis direction, and the electric field intensity radiation directions for transmission and reception are different when the antennas are placed at right-angles to each other.

The electric field intensity pattern in the air reflects that in pure water. The $S_{21}$ value observed at frequencies below 1 GHz is due to omnidirectional signal transmission and reception using the cylindrical enclosure (ABS resin) of the water antenna as an antenna. It is considered to vary with the material and structure of the enclosure.

The 2.4 GHz patch antenna shows higher-order mode current density distribution and electric field intensity radiation pattern at 3.5 GHz (Figure 6). The signal pin length of the monopole water antenna was shortened to about 4 mm so that signals in the higher-order mode at 3.5 GHz could be received by the monopole water antenna (Figure 3). As shown in Figure 6, the higher-order mode of the 2.4 GHz patch antenna exhibits an electric field intensity radiation pattern that is 90 degrees different from that of the fundamental mode. Therefore, the 3.5 GHz transmission coefficient $S_{21}$ has a low value when received by a 3.5 GHz monopole water antenna placed opposite the 2.4 GHz patch antenna in the forward direction along the X axis. When the 3.5 GHz monopole water antenna was rotated 90 degrees relative to the 2.4 GHz patch antenna, the receiving sensitivity at 3.5 GHz was improved by about 9 dB (Figure 11). When a 3.5 GHz monopole antenna is placed opposite the 2.4 GHz patch antenna in the forward direction, the signal reception is possible over a wide frequency range from 1 to 5 GHz. However, the overall reception sensitivity is very low. Shortening the signal pin length of a monopole water antenna can extend the transmission and reception frequency range, but this is a trade-off for reducing receiver signal sensitivity.

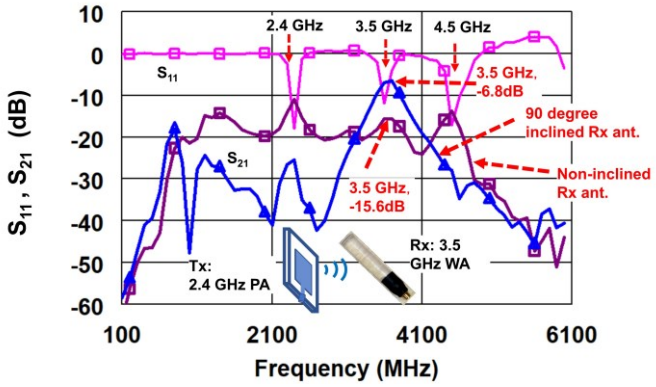


Fig. 11. Measured reflection coefficient $S_{11}$ and transmission coefficient $S_{21}$ with 2.4 GHz band patch antenna (transmitter) and 3.5 GHz band monopole antenna (receiver)

## VI. $S_{21}$ TRANSMISSION COEFFICIENT MEASUREMENTS FOR THE DISTANCE BETWEEN TRANSMITTING AND RECEIVING 2.4 GHZ MONOPOLE WATER ANTENNAS

We measured the transmission coefficient $S_{21}$ for a 2.4 GHz monopole water antenna ($L_{WA}$ = 50 mm) with different distances $L_{AIR}$ between transmitter and receiver. The measurement results are shown in Figure 12. The equation for the measured values of $S_{21}$ is given in (1), and the constant K is given in (2). The value of $S_{21}$ decreases with the square of the distance $L_{AIR}$, reflecting the spatial propagation attenuation characteristics of the electromagnetic wave. The $S_{21}$ value is approximately 10 dB lower than the 2.4 GHz patch antenna. The reason for the lower transfer coefficient is the lower antenna gain due to the omnidirectional nature of the monopole water antenna compared to the highly directional patch antenna. Other possible factors are the low electric field intensity coupling between the electrode pin of the monopole water antenna and the pure water and the low-radiation efficiency of the electromagnetic power from the pure water to the air.

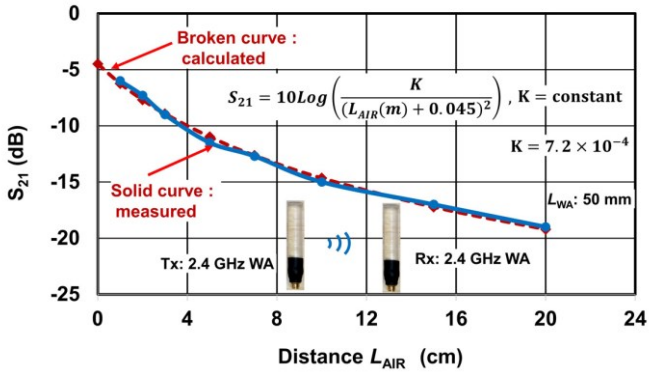


Fig. 12. Transmission coefficient measurement at different distances between the transmitter and receiver of the 2.4 GHz band monopole water antennas

$$S_{21} = 10\log\left(K/\{L_{AIR}(m) + 0.045\}^2\right) \quad (1)$$

$$K = 7.2 \times 10^{-4} \quad (2)$$

## VII. Consideration of the Operating Mechanism of Monopole Water Antennas

We discuss the operating mechanism and antenna characteristics of monopole water antennas. As shown in Figure 13, the electrical signal is fed to the electrode pin through the external connector applies an electric field to the water molecules inside the capsule by generating an electric field between the ground on the bottom of the electrode pin and the electrode pin. The water molecule is a protonic polarized molecule with the highest polarization in liquids [29] and can be considered a dipolarized element [27]. When the electrical signal input to the electrode pin is a high-frequency signal, the applied electric field causes the dipole polarization element to move, rotate, and vibrate. The electromagnetic field generated by the movement, rotation, and vibration of the dipolarized elements is applied to the neighboring dipolarized elements, and high-frequency signals are propagated through the water molecules ($H_2O$) in the capsule. The electromagnetic field generated by this dipole polarizing element (polarized water molecules) is radiated outside the capsule and acts as an antenna.

In addition, depending on the intensity and frequency of the high-frequency signal inside the capsule and the state of the water molecules, the protons and electrons of the polarized molecules are released, drift, and vibrate to generate an electromagnetic field. The formation of hydrated ions such as NaCl and the polymerization of water molecules in the capsule causes collisions and scattering with polarized $H_2O$ molecules, protons, and electrons. Hence it decreases antenna efficiency and increases noise figure. At lower frequencies, it is also affected by the complex permittivity of the capsule enclosure material.

The operating mechanism of the water antenna is expected to be the same even if the monopole antenna part is replaced by a planar or three-dimensional antenna (such as an F-shaped or a helical antenna).

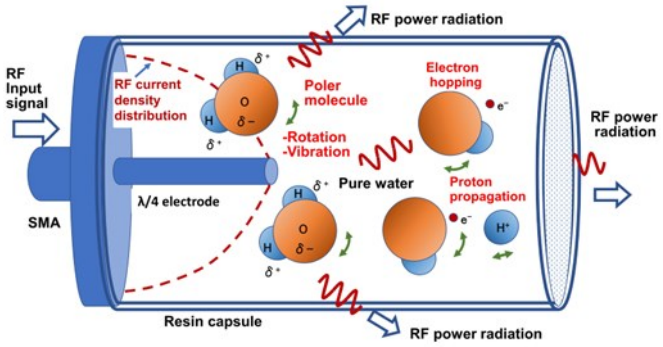


Fig. 13. A working mechanism of monopole water antenna

## VIII. Conclusion

A 2.4 GHz band monopole water antenna with a monopole electrode and SMA connector, which has the basic structure of an antenna, was designed, fabricated, and mounted in a resin capsule filled with pure water. In the monopole water antenna design, the S-parameter's reflection coefficient $S_{11}$ and transmission coefficient $S_{21}$ were investigated using an electromagnetic field simulator AXIEM. The S-parameters were measured using a portable vector network analyzer, and an LNA with 20 dB gain in the 0.1-7 GHz band designed and fabricated with a single SiGe bipolar stage was used to amplify the received signal. A narrowband, directional 2.4 GHz patch antenna was designed and fabricated to compare measurements from a monopole water antenna. The measured and simulated frequency characteristics of the monopole electrode pin length (3-8 mm) and the reflection coefficient $S_{11}$ are almost in agreement, and an electrode pin length of 8 mm at 2.4 GHz and 4 mm at 3.5 GHz were obtained. The current density distribution, electric field intensity radiation pattern ($E_\theta$, $E\varphi$), and reflection coefficient $S_{11}$ of the 2.4 GHz patch antenna included a 2.4 GHz fundamental mode ($TE_{10}$) and a 3.5 GHz higher order mode ($TE_{02}$), whose polarization directions were 90 degrees different. Two types of monopole water antennas with the same polarization direction but different frequencies (2.4 GHz and 3.5 GHz) were compared. The 2.4 GHz monopole water antenna received only the fundamental mode signals from the patch antenna. By rotating the 3.5 GHz monopole antenna by 90 degrees, the patch antenna's 3.5 GHz higher-order mode signal was received. The $S_{21}$ values measured for different transmit-receive distances between the transmission and reception of the 2.4 GHz monopole water antenna decreased with the square of the antenna distance, similar to the spatial propagation characteristics of electromagnetic waves. The same results are expected to be obtained by replacing the monopole electrode with a planar or three-dimensional antenna [6, 8, 17, 21, 23]. This research method can be applied to seawater and freshwater wireless communication and biotechnology fields [4, 7, 10, 22].

## References

[1] S. W. Maley and R. J. King, "Impedance of a Monopole Antenna With a Circular Conducting-Disk Ground System on the Surface of a Lossy Half Space l," *Journal of Research of the Notional Bureau of Standards - D. Radio Propagation*, vol. 65D, no.2, pp. 183-188, 1961

[2] G. Ruvio, D. Gaetano, M. J. Ammann, and P. McEvoy, "Antipodal Vivaldi Antenna for Water Pipe Sensor and Telemetry," *Hindawi Publishing*

*Corporation International Journal of Geophysics*, vol. 2012, article ID 916176, 8 pages, 2012.

[3] H. Changzhou, S. Zhongxiang, "High efficiency seawater monopole antenna for maritime wireless communications," *IEEE Transactions on antennas and propagation*, 62(12), pp. 5968-5973. pp. 1-9, 2013. https://doi.org/10.1109/TAP.2014.2360210

[4] E.M. Cheng, M. Fareq, Shahriman A. B., Mohd Afendi R., Y. S. Lee, S. F. Khor, W.H. Tan1, M. N. N. Fazli., A. Z. Abdullah, and M. A. Jusoh, "Development of Microstrip Patch Antenna Sensing System for Salinity and Sugar Detection in Water," *International Journal of Mechanical and Mechatronics Engineering*, vol. 14, no. 05, pp. 31-36, 2014.

[5] L. Xing, Y. Huang, Y. Shen, S. Aliaafreh, Q. Xu, and R. Alrawashdeh, "Further investigation on water antennas," *IET Microw. Antennas Propag.*, vol. 9, is. 8, pp. 735-741, 2015.

[6] Y. Li and K. Luk, "A Water Dense Dielectric Patch Antenna," *IEEE Open Access Journal*, vol. 3, pp. 274-280, 2015.
https://doi.org/10.1109/ACCESS.2015.2420103

[7] X. Yan and X. Zhang, "Decoupling and matching network for monopole antenna arrays in ultrahigh field MRI," *Quant Imaging Med Surg*., 5(4), pp. 546-551, 2015. https://doi.org/10.3978/j.issn.2223-4292.2015.07.06

[8] L. Xing, Y. Huang, Q. Xu, and S. Aliaafreh, "A Wideband Hybrid Water Antenna with an F-Shaped Monopole," *IEEE Access*, 2461443, pp. 1179-1187, 2015. https://doi.org/10.1109/ACCESS.2015.2461443

[9] M. Zou, Z. Shen, and J. Pan, "Frequency-reconfigurable water antenna of circular polarization," *Applied Physics Letters*, 108, 014102, pp. 1-9, 2016.

[10] M. T. Islam, M. N. Rahman, M. S. J. Singhi, and M. Samsuzzaman, "Detection of Salt and Sugar Contents in Water on the Basis of Dielectric Properties Using Microstrip Antenna-Based Sensor," *IEEE Access*, vol. 6, pp. 4118-4126, 2017.

[11] T. D. Paillette, A. Gaugue, E. Parlier, and S. Dardenne, "Antenna Design for Underwater Wireless Telemetry Systems," *11th European Conference on Antennas and Propagation (EUCAP)*, EuCAP. 2017.928513, 2017. https://doi.org/10.23919/EuCAP.2017.7928513

[12] V. Hemamalini, R. K. Prathesha, M. M. Sumithra, and P. Nandhini, "Design of Submarine Monopole Antenna For Data Transmission," *International Journal of Advanced Research in Electrical, Electronics and Instrumentation Engineering*,vol. 6, iss. 3, pp.1649-1653, 2017.

[13] K. O. Joseph, E. Karthika, M. Keerthika, and G. Mugashini, "High-Efficiency Sea-Water Monopole Antenna for Maritime Wireless Communications," *International Journal of Scientific Development and Research (IJSDR)*, vol. 2, iss. 4, pp. 104-108, 2017. https://doi.org/10.1109/TAP.2014.2360210

[14] Z. P. Zhong, J. J. Liang, G. L. Huang, and T. Yuan, "A 3D-Printed Hybrid Water Antenna with Tunable Frequency and Beamwidth," *Electronics* 2018, 7, 230; electronics 7100230, pp. 1-13, 2018.

[15] X. Chen, "Research on Simulation and Calculation of a New Reconfigurable Sea Water Antenna," *Advances in Computer Science Research*, vol. 86, pp. 334-339, 2018.

[16] I. I. Smolyaninov, Q. Balzano, C. C. Davis, and D. Young, "Surface Wave Based Underwater Radio Communication," *IEEE Antennas and Wireless Propagation Letters*, vol. 17, no. 12, pp. 2503-2507, 2018. https://doi.org/10.1109/LAWP.2018.2880008

[17] C. Song, E. Bennett, J. Xiao, Q. Hua, L. Xing, and, Y. Huang, "Compact Ultra-Wideband Monopole Antennas Using Novel Liquid Loading Materials," *IEEE Open Access Journal*, vol. 7, pp. 49039-49047, 2019.

[18] N. H Moktar, W. I Roseli, M. T Ali, and N. H. A. Rahman, "Analysis of Water Dense Dielectric Patch Antenna utilizing Six Different Waters for Wireless Applications," *2019 International Symposium on Antennas and Propagation (ISAP)*, 19284192, 2019.

[19] L. Xing, J. Zhu, Q. Xu, D. Yan, Y. Zhao, "A Circular Beam-steering Antenna with Parasitic Water Reflectors," *IEEE Antennas and Wireless Propagation Letters*, vol.18, is. 10, pp. 2140-2144, 2019. https://doi.org/10.1109/LAWP.2019.2938872

[20] D. T. Phan and C. W. Jung, "Optically transparent sea-water monopole antenna with high radiation efficiency for WLAN applications," *Electronics Letters*, vol. 55, no. 24, pp.1269-1271, 2019. https://doi.org/10.1049/el.2019.2664

[21] J. Sun and K. Luk, "A Compact-Size Wideband Optically-Transparent Water Patch Antenna Incorporating an Annular Water Ring," *IEEE Access*, vol.7, pp.122964-122971, 2019.
https://doi.org/10.1109/ACCESS.2019.2936458

[22] S. L. Baika, S. S. Thakur, and V. C. Kshirsagar, "Printed Ring Monopole Antenna for Medical Application," *JETIR*, vol. 6, is. 5, pp. 747-749, 2019.

[23] J. Majcher, M. Kafarski, A. Wilczek, A. Woszczyk, A. Szypowska, A. Lewandowski, J. Szerement, and W. Skierucha, "Application of a Monopole Antenna Probe with an Optimized Flange Diameter for TDR Soil Moisture Measurement," *Sensors*, 20, 2374, pp. 1-13, 2020. https://doi.org/10.3390/s20082374

[24] R. E. Jacobsen, A. V. Lavrinenko, and S. Arslanagic, "A Water-Based Huygens Dielectric Resonator Antenna," *IEEE Open Access Journal and Propagation,* pp. 493-499, 2020.
https://doi.org/10.1109/OJAP.2020.3021802

[25] Y. Huang, L. Xing, C. Song, S. Wang, and F. Elhouni, "Liquid Antennas: Past, Present and Future," *IEEE Open Journal of Antennas and Propagation,* vol. 2, pp.473-487, 2021.
https://doi.org/10.1109/OJAP.2021.3069325

[26] C. Hua, S. Wang, Z. Hu, Z. Zhu, Z. Ren, W. Wu, and Z. Shen, "Reconfigurable Antennas Based on Pure Water," *IEEE Open Journal of Antennas and Propagation,* vol. 2, pp. 623-632, 2021. https://doi.org/10.1109/OJAP.2021.3079353

[27] K. Chinen, S. Nakamoto, and I. Kinjo, "Two-port Equivalent Circuits Deduced from S-parameter Measurements of NaCl Solutions," *IETE Journal of Research*, 05 Jun. IF 1.877, pp. 1-9, 2022. https://doi.org/10.1080/03772063.2022.2081264

[28] Axiem, "awr-awr-axiem-analysis,"
https://www.cadence.com/home/tools/system-analysisrf-microwave-design/awr-axiem-analysis.html

[29] Sodex, "Polarities of Solvents,"
https://wwww.shodex.com/ja/dc/06/0117.html